Separation Science and Technology
Publication details, including instructions for authors and subscription information:
http://www.informaworld.com/smpp/title~content=t713708471

Magnetic Carrier for Radionuclide Removal from Aqueous Wastes: Parameters Investigated in the Development of Nanoscale Magnetite Based Carbamoyl Methyl Phosphine Oxide

R. D. Ambashta[a]; P. K. Wattal[a]; S. Singh[b]; D. Bahadur[c]
[a] Backend Technology Development Division, Bhabha Atomic Research Centre, India [b] Solid State Physics Division, Bhabha Atomic Research Centre, India [c] Department of Metallurgical Engineering and Materials Science, Indian Institute of Technology, Bombay, India

To cite this Article Ambashta, R. D. , Wattal, P. K. , Singh, S. and Bahadur, D.(2006) 'Magnetic Carrier for Radionuclide Removal from Aqueous Wastes: Parameters Investigated in the Development of Nanoscale Magnetite Based Carbamoyl Methyl Phosphine Oxide', Separation Science and Technology, 41: 5, 925 — 942
To link to this Article: DOI: 10.1080/01496390500528033
URL: http://dx.doi.org/10.1080/01496390500528033

Separation Science and Technology, 41: 925–942, 2006

ISSN 0149-6395 print/1520-5754 online
DOI: 10.1080/01496390500528033

Magnetic Carrier for Radionuclide Removal from Aqueous Wastes: Parameters Investigated in the Development of Nanoscale Magnetite Based Carbamoyl Methyl Phosphine Oxide

R. D. Ambashta and P. K. Wattal
Backend Technology Development Division,
Bhabha Atomic Research Centre, India

S. Singh
Solid State Physics Division, Bhabha Atomic Research Centre, India

D. Bahadur
Department of Metallurgical Engineering and Materials Science,
Indian Institute of Technology, Bombay, India

Abstract: A study on superparamagnetic magnetite polymer composite development was undertaken for application to magnetically assisted chemical separation. Tetramethyl ammonium hydroxide as an alternative to ammonia was used as a precipitation agent to obtain nanoscale magnetite particles. Investigation on stoichiometry control of Fe(III) and Fe(II) ions suggested a correlation between alkalinity and initial Fe(III): Fe(II) ratio for precipitation of magnetite. Studies on polymerization conditions suggested that polymers setting at ambient conditions enable retention of superparamagnetic property of substrate magnetite. Vaporization method for

Received 20 September 2005, Accepted 5 December 2005
Address correspondence to R. D. Ambashta, Backend Technology Development Division, Bhabha Atomic Research Centre, India. E-mail: aritu@magnum.barc.ernet.in

impregnation of solvent extractant CMPO, yielded product that had a high sorption capability for radionuclide europium as compared to wet impregnation method.

Keywords: Magnetic carrier, radionuclide removal, nanoscale magnetite particles, carbomoyl methyl phosphine oxide

INTRODUCTION

In order to achieve as low as reasonably achievable (ALARA) discharge limit from nuclear plant sites, radioactive liquid wastes generated at these sites need to be subjected to treatment systems such as column-based ion exchange and density-based solvent extraction separation. Magnetically assisted chemical separation (MACS) (1–3) is emerging as a common separation technology for radionuclide removal from nuclear wastes that utilizes low inventory of solvents and exchangers. In high gradient magnetic filtration (HGMF) techniques, particles with a diameter larger than superparamagnetic limit exhibit an undesirable "magnetic memory" after being exposed to an applied magnetic field. This hinders the magnetic filter regeneration procedure. For HGMF applications, it is therefore, desirable to have superparamagnetic behavior at room temperature. Single domain particles, whose thermal energy is greater than or equal to the magnitude of magnetic anisotropy energy barrier, exhibit superparamagnetic relaxation (4). Superparamagnetic magnetite (Fe_3O_4) particles enable efficient filter regeneration capability. The support matrix within which nanostructures are synthesized determine their physical properties in addition to providing a means of particle dispersion (5).

Octyl (phenyl) carbamoyl methyl phosphine oxide (CMPO) has been studied extensively for the separation of transuranics (6–8). For application to MACS, polymer coated superparamagnetic magnetite particles have been studied as substrates to CMPO for removal of lanthanides and actinides from liquid wastes (9). We have studied different parameters in the development of novel magnetic carriers for removal of europium from aqueous medium. Magnetite is a common substrate studied extensively in magnetically assisted chemical separation applications which can be prepared from precipitation of a mixture of Fe(III) and Fe(II) in molar stoichiometric proportions of 2:1 (10). Ammonia is among common precipitation agents used for the purpose (11). Owing to the low boiling point (38°C) and high vapor pressure (48 kPa at 20°C) of ammonia; it has limitations for industrial scale up. Tetramethyl ammonium hydroxide, on the other hand, has a vapor pressure of 2.3 kPa at 20°C and boils at 100°C. In addition it serves as dispersion agent to obtain nanoparticles of magnetite (12). We have studied the influence of initial stoichiometry of iron for superparamagnetic magnetite precipitation under high alkaline conditions of tetramethyl ammonium hydroxide. We have also studied the influence of polymerization

conditions on magnetic properties of magnetite. Different solvent mixtures of CMPO, tributyl phosphate (TBP), n-dodecane, and ethanol and different impregnation methods of these solvents were studied for maximum uptake of radionuclide europium at magnetite polymer composite surface.

EXPERIMENTAL

Iron Oxide

Hydrophobically coated iron oxide particles were prepared in water in toluene dispersion. Iron (III) chloride (2 M, 26 mL), iron (II) chloride (0.5 M, 52 mL), toluene (130 mL), tetramethyl ammonium hydroxide (25% in methanol, 78 mL), cetyl trimethyl ammonium bromide (0.6 g), and styrene monomer (1 g), were mixed under sonication. The molar ratio of Fe(III):Fe(II) was 2:1 in this composition. In the second set, the molar ratio of Fe(III):Fe(II) was maintained as 1:1, with Fe(III) chloride (1 M, 26 mL) and Fe(II) chloride (0.5 M, 52 mL). The volume proportions of other components were kept unchanged.

Magnetite Polystyrene

A continuous fluid phase was formed from water and polyvinyl alcohol. About 600 g of deionized water was weighed into a 2 L, four-necked round-bottom flask fitted with a condenser; nitrogen inlet, an overhead stirrer, and a separating funnel to introduce fluids. The flask was immersed in a water bath and the bath temperature set to 90°C. The water in the flask was purged with nitrogen for 30 minutes. About 6 g of polyvinyl alcohol (molecular weight: 22000) was added to the flask; a nitrogen blanket is maintained above the liquid surface for the duration of the reaction. The continuous fluid phase was stirred for 30 minutes at 90°C, and allowed to cool (with stirring) to 65°C for about 16 h. Separately, the dispersed phase was formulated from primary hydrophobically coated magnetite beads, styrene (19 g), dimethyl aniline (accelerator, 20 μL) and benzoyl peroxide (initiator, 0.2 g) by mixing under nitrogen for 20 minutes. This mixture was poured into the continuous fluid phase, pre-cooled to room temperature and stirring was continued. Reaction was allowed to proceed for 24 h at 80°C temperature. The particles were collected on magnet, supernatant discarded. These were washed about five times with methanol and water in proportion 9:1 by volume and finally with water.

Magnetite Polyester Polystyrene

Instead of styrene monomer, polyester in styrene monomer was added for the preparation. The polyester used was a derivative of propylene glycol,

isophtalic acid, and maleic anhydride. The experimental assembly remained the same as for magnetite polystyrene but reaction was pursued at room temperature.

Solvent Extractant Impregnation

"Wet impregnation" and "impregnation by vaporization of diluent" methods were adopted for the loading of extractant to magnetite polyester polystyrene beads. In the wet impregnation method, the extractant was contacted with the beads in the ratio 10:1 by weight and allowed to stand for 24 h. In this method, the influence of diluents and phase modifiers on the extractant loaded magnetic beads was studied for three mixture-types with CMPO in different concentrations. The details of the proportions are given in Tables 1 and 2. Mixture I comprised of CMPO, TBP, and n-dodecane. In mixture Ia, the relative molar proportion of CMPO and TBP were fixed as 0.25:1.2 but the total amount was varied with respect to n-dodecane. In mixture Ib, TBP concentration was fixed and CMPO concentration was gradually increased. Mixture II comprised of CMPO in n-dodecane in the absence of TBP. Mixture III comprized of CMPO in ethanol in the proportion 1:10 by volume. This was heated at 40°C under nitrogen for 24 h to ensure evaporation of alcohol. The proportion of extractant to bead was maintained at 10:1 by weight. The solvents were pre-equilibrated with nitric acid (2 N) in volume proportions of 1:1 before contacting with the beads. The equilibration step included shaking solvents with nitric acid for 15 minutes followed by standing for 24 h.

Table 1. Distribution coefficients of mixture I comprising of CMPO (extractant), TBP (phase modifier) and n-dodecane (diluent)

Sample	CMPO(M)	TBP(M)	$K^{a}_{d,\ Eu}$
Mixture Ia			
1.	0.25	1.20	10.01
2.	0.30	1.44	10.14
3.	0.40	1.92	13.91
4.	0.50	2.40	13.75
Mixture Ib			
5.	0.25	1.20	9.85
6.	0.50	1.20	10.21
7.	1.00	1.20	10.19
8.	1.50	1.20	100

[a]Standard deviation is between 4–8%.

Table 2. Mixture II comprising of CMPO (extractant) and n-dodecane (diluent)

CMPO (M)	CMPO (% by volume)
0.2	10
0.6	30
1.2	50
1.5	70
1.9	90
Absolute	100

Characterization

Crystallographic structures of samples were examined by X-ray diffractometer using copper K_α source operating at 40 KV/30 mA. The samples were scanned at a scan rate of about 0.1° per minute. The samples were indexed to Miller planes using Bragg's law (13). Philips Model CM200 TEM, operating at 180 keV, was used for imaging the samples. A selected area electron diffraction (SAED) on the particles was carried out for the samples. The samples were indexed to Miller planes using methods of ratios (14). For analysis of iron content in the magnetic polymer beads, the sample was first mixed with twice the amount of potassium bisulphate by weight and fired in platinum crucible under oxidizing flame. The residue was dissolved in hot concentrated nitric acid. Iron estimation was followed by a treatment of solution with ammonium thiocyanate to form iron thiocyanate. Calibration with respect to standard iron solutions was used to estimate the concentration of iron in the present sample by measuring absorbance of iron thiocyanate complex at 565 nm using an ultraviolet-visible spectrometer (UV-160A Shimadzu). The dc magnetization measurements were carried out using 12 Tesla (Oxford Instruments) vibrating sample magnetometer as a function of magnetic field and temperature. For zero field cooled magnetization (M_{ZFC}) measurements, the sample was first cooled from room temperature down to 5 K in zero field. After applying 100 Oe field at 5 K, the magnetization was measured in the warming cycle. Whereas, for field cooled magnetization (M_{FC}) measurements, the sample was cooled in the same field (100 Oe) down to 5 K and the magnetization was measured in the warming cycle under the same field. Mössbauer spectra were recorded with a 50 mCi ^{57}Co in Rh source at 300 K. Each spectrum was folded with respect to calibration spectrum of α-iron using Recoil Demo (Mössbauer Analysis Software) program and shift velocity parameters were determined. The hydrodynamic diameter was obtained by using a Zeta-sizer unit (Malvern-make). Samples were dispersed in water-calcon, sonicated, and analyzed for particle size distribution.

Radionuclide Uptake Behavior

The solvent mixture compositions described in Tables 1 and 2 were studied with europium tracer. For the studies, 1.5 mL of europium tracer ($^{152-154}$Eu $\sim$ 100 Bq/mL) was contacted with 30 mg of CMPO loaded magnetic beads [This was prepared by dilution from a stock of $\sim$35 MBq/mL $^{152-154}$Eu in sample HCl at pH 2. The specific activity of stock sample was $\sim 3.7 \times 10^{10}$ Bq/g Eu.]. The solution after 15 minutes equilibration time was held on a magnet and supernatant was assayed for europium radioactivity using a sodium iodide (thallium) based gamma detector. The beads in the absence of extractant were similarly contacted with europium and solution was assayed for activity before and after equilibration. In order to determine the sorption capability of the sorbent, the concentration of Eu in nitric acid (2 N) was progressively varied from $\sim 10^{-6}$ M to 0.1 M. The sorbents were separated using magnetic assistance. All extraction studies were carried out at 300 K.

The sorption behavior for a radionuclide was studied in terms of the distribution coefficient parameter (K_d), which relates the concentration of solute species taken by sorbent medium from the solution. It is expressed as

$$K_d = \left(\frac{C_i - C_f}{C_f}\right) \times \frac{V}{m} \tag{1}$$

where C_i and C_f are the concentrations of the solute in aqueous medium before and after equilibration, V is the volume of solution and m is mass of magnetic particle used as exchanger or extractant. In case of radionuclide assaying, the concentration is directly proportional to the counts of gamma radiation. The detector used for the counting was sodium iodide-thallium based scintillation detector. The expression used in the studies was therefore

$$K_d = \left(\frac{A_i - A_f}{A_f}\right) \times \frac{V}{m} \tag{2}$$

where A_i and A_f are the activities of the radionuclide in the aqueous medium, before and after equilibration, V and m have been defined above. The standard deviation in distribution coefficient was evaluated as

$$\sigma_{K_d} \equiv \frac{V}{m} \times \frac{(A_i - A_f)}{A_f} \times \sqrt{\left(\frac{(A_i + A_f)}{(A_i - A_f)^2} + \frac{1}{A_f}\right)} \tag{3}$$

where σ_{K_d} is the standard deviation of distribution coefficient. The other variables have been defined before.

RESULTS AND DISCUSSION

The stoichiometry of Fe(III) to Fe(II) was varied as 2:1 and 1:1 moles to ascertain the right stoichiometry needed for magnetite precipitation. With the Fe(III):Fe(II) ratio maintained as 2:1, a brownish red compound formed. The XRD patterns of the samples are shown in Fig. 1a. Two major lines corresponding to (104) and (110) planes of rhombohedral α-Fe_2O_3 (JCP-PDF no. 33-0664) are observed in the pattern. The line corresponding to (110) plane is common to line corresponding to (311) plane of Fe_3O_4. With the Fe(III):Fe(II) ratio maintained as 1:1, a black precipitate formed. Five major lines corresponding to (220), (311), (400), (511), and (440) planes of face centred cubic Fe_3O_4 are observed in Fig. 1b.

A comparison of the magnetization behavior of samples (DC magnetization M versus applied field H) is shown in Fig. 2. Inset shows magnetization for sample prepared from Fe(III):Fe(II) = 2:1, on an enlarged scale. For the sample prepared from initial stoichiometry of Fe(III): Fe(II) = 2:1, the

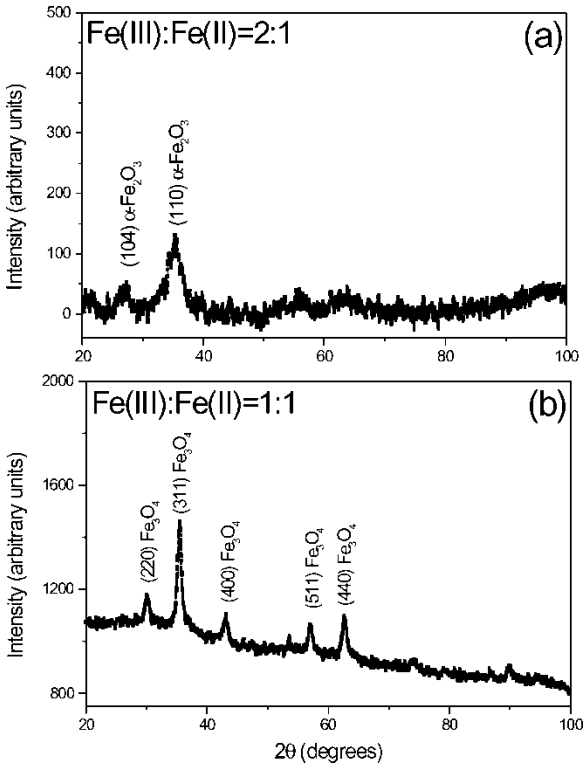

Figure 1. X-ray diffraction pattern of iron oxide obtained from variation in initial molar ratio of Fe(III):Fe(II) as (a) 2:1 and (b) 1:1.

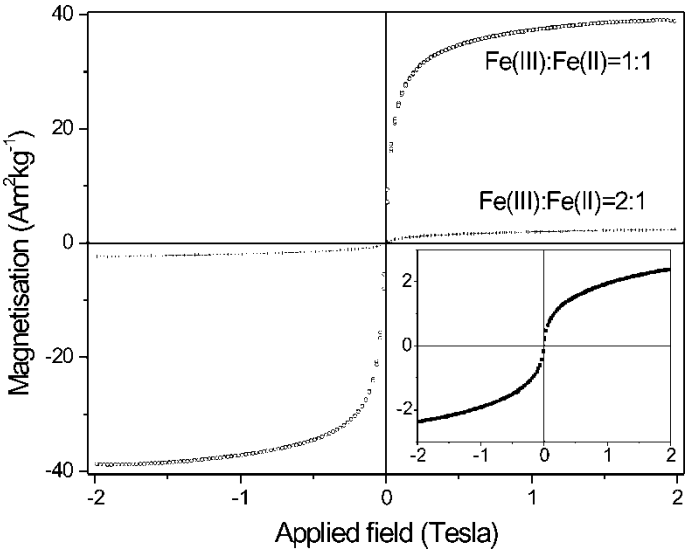

Figure 2. *M* v/s *H* plot for iron oxide obtained from variation in initial molar ratio of Fe(III):Fe(II) as 2:1 and 1:1. Inset shows *M* v/s *H* plot for ratio 2:1 on an enlarged scale.

magnetization values are high as compared to pure α-Fe_2O_3 (antiferromagnetic compound); therefore admixture presence with Fe_3O_4 is also inferred from the observations. Coercivity is a measure of resistance to demagnetization. Absence of coercivity and non-saturation of *M* versus *H* curve confirm the superparamagnetic nature of sample prepared from initial molar ratio of Fe(III):Fe(II) =2:1. For the sample prepared from initial stoichiometry of Fe(III):Fe(II) = 1:1, a small coercivity of $\sim$0.3 kA/m was observed.

For the precipitation of magnetite, when the molar Fe(II) and Fe(III) ions are in stoichiometric proportion, the ideal pH is 7. Gribanov and coworkers (15) showed that strong alkali such as KOH and NaOH shift the pH of the mixture to $\sim$14, leading to formation of large quantity of complexes which form the basis for formation of nonmagnetic hydrated forms of iron ($HFeO_2^-$ for the divalent iron and $Fe(OH)_4^-$ and $FeO(OH)_2^-$ for the trivalent one). Thus the probability of Fe_3O_4 formation reduces with the use of strong alkali. Gokon and coworkers (16) have studied the influence of iron stoichiometry on Fe_3O_4 formation in the presence of a magnetic field. When the Fe(III):Fe(II) ratio was taken as 2:1, Fe_3O_4 formation was via Fe(III)Fe(II)hydroxide polymer intermediate that transformed to Fe_3O_4. With Fe(III):Fe(II) = 1:2, Fe_3O_4 formation was via soluble intermediate Fe(III)Fe(II)oxohydroxochloro intermediate complex. Tamaura and coworkers (17) have suggested a two-step mechanism, where an intermediate of γ-FeOOH or green rust formed by the oxidation of Fe(II) ions followed by their transformation to Fe_3O_4. Kiyama (18) has shown that rust formation on

mild steel lead to Fe(II)oxohydroxide formation that on further oxidation transformed to Fe_3O_4. This is also an example of nonstoichiometric iron source conversion to Fe_3O_4 form.

In our studies, the pH of solution used for precipitation from Fe(III) and Fe(II) mixed chloride was ~13. Tetramethyl ammonium hydroxide being a strong alkali, dissociates into tetramethyl ammonium ion and hydroxide ion. The molar ratio of Fe(III) to Fe(II), when taken as 1:1, forms an aqueous mixed iron hydroxo chloride salt, which transforms to Fe_3O_4. In the hydrophobically coated magnetite preparation step, monomer is sonicated in the water toluene dispersion. Ultrasonication is capable of producing cavitation, which serves as a means of concentrating the diffused energy of sound into a unique set of conditions that can concentrate radicals. The sources of radicals can be H and OH of water. These catalyze radical formation in monomer (19). Radical formation during sonication could have facilitated Fe(II) oxidation. With initial Fe(III):Fe(II) in proportion of 2:1, this could have caused formation of major non magnetic Fe(III) oxide and with initial Fe(III):Fe(II) in proportion 1:1, Fe(II) oxidation helped in transformation of Fe(II)-Fe(III) oxo-hydroxo-chloro green complex to Fe_3O_4. The proportion of Fe(III):Fe(II)=1 was therefore maintained for the preparation of composites with polymers.

The photograph of TEM image of magnetite polystyrene composite, shown in Fig. 3, indicates the clustering of the particles in the polymer matrix. The selected area electron diffraction pattern of the sample shows the presence of a face-centred cubic structure, characteristic of magnetite structure (20). The photograph of TEM image of the polyester polystyrene-loaded magnetite beads is shown in Fig. 4. The diffused nature of the diffraction pattern may be considered as evidence of coating of polymer on magnetite. Field (H) dependence of DC magnetization (M) of magnetite polystyrene and magnetite polyester polystyrene at 300 and 5 K are shown in Fig. 5 and 6, respectively. The saturation magnetization of magnetite

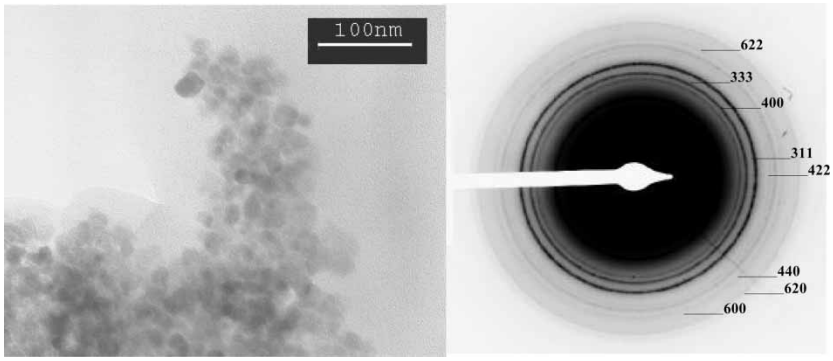

Figure 3. TEM image of magnetite polystyrene and selected area diffraction pattern.

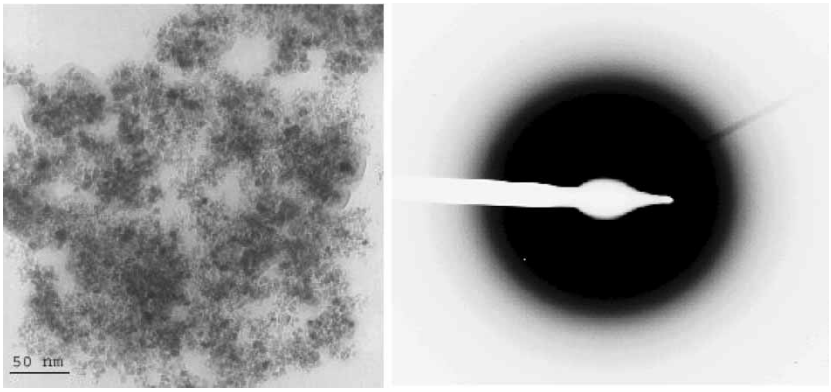

Figure 4. TEM image of magnetite polyester polystyrene and selected area electron diffraction pattern.

polystyrene was observed from 5 K data as 56.5 Am^2kg^{-1} and magnetite polyester polystyrene as 9 Am^2kg^{-1}. The magnetite content on iron assay was evaluated as 45% by weight for magnetite polystyrene and 12% by weight for magnetite polyester polystyrene. Figure 7 depicts the temperature dependence of zero field magnetization (M_{ZFC}) and field cooled magnetization (M_{FC}) for magnetite polystyrene under an applied field of 100 Oe. The M_{ZFC} and M_{FC} curves do not overlap with each other at any point in the temperature range of 10 to 300 K. This feature is typical of a broad distribution of particle size (21). When polymerization is pursued at high temperature, the magnetite crystallites grow in size. Magnetization is considerably enhanced

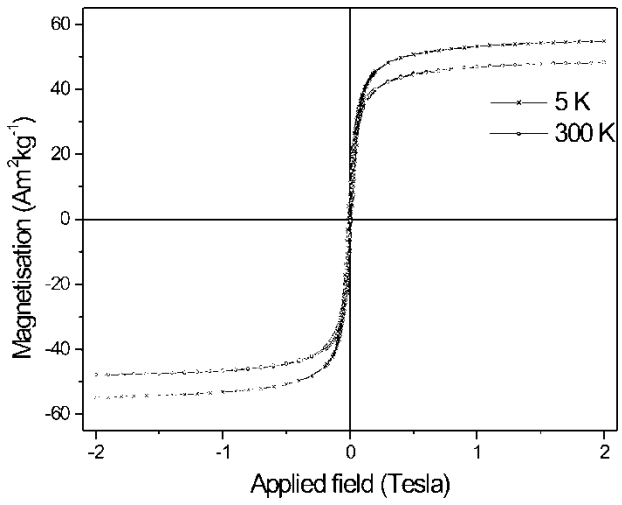

Figure 5. *M* v/s *H* plot for magnetite polystyrene at 300 K and 5 K.

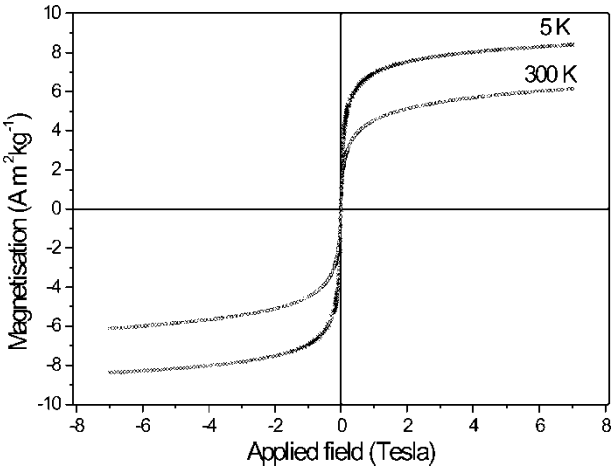

Figure 6. *M* v/s *H* plot for magnetite polyester polystyrene at 300 K and 5 K.

and the particles are no longer superparamagnetic as evidenced by the nature of the M_{FC}-M_{ZFC} curve. Figure 8 depicts the temperature dependence of M_{ZFC} and M_{FC} for magnetite polyester polystyrene. Nature of curve indicates that majority of the particles are superparamagnetic in nature at 300 K.

Broadened hyperfine splitting in the spectrum shown in Fig. 9 is the Mössbauer spectrum of magnetite polystyrene indicating strong interparticle

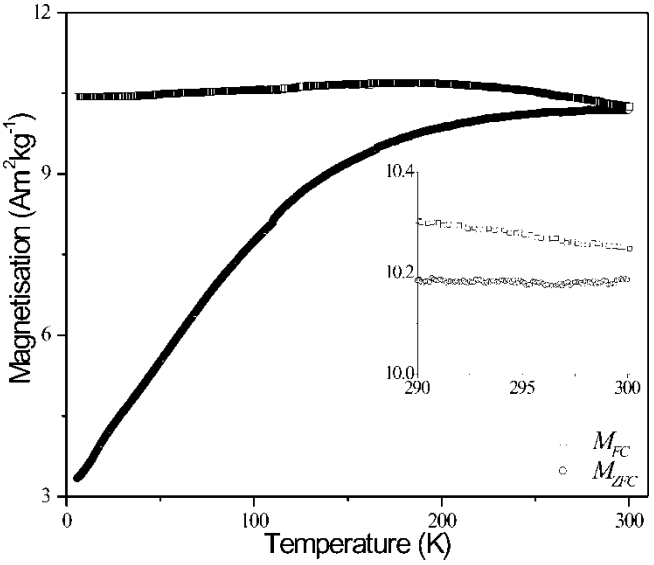

Figure 7. M_{FC}-M_{ZFC} plot for magnetite polystyrene.

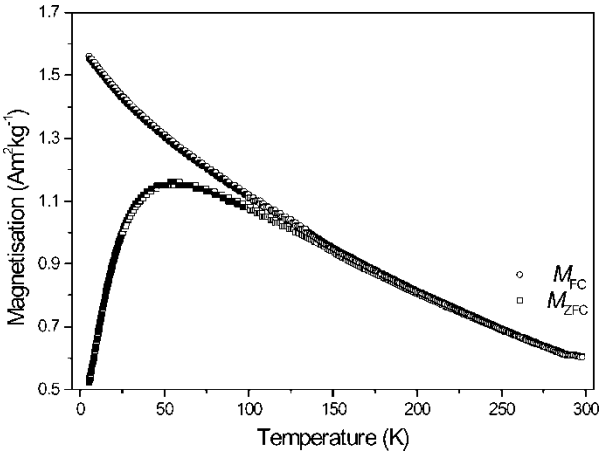

Figure 8. M_{FC}-M_{ZFC} plot for magnetite polyester polystyrene.

magnetic interactions in magnetite polystyrene. The Mössbauer spectrum of magnetite polyester polystyrene, shown in Fig. 10 primarily consists of a major quadruople doublet, characteristic of superparamagnetic Fe_3O_4. The Mössbauer spectrum of ordered magnetite sample consists of three sextets

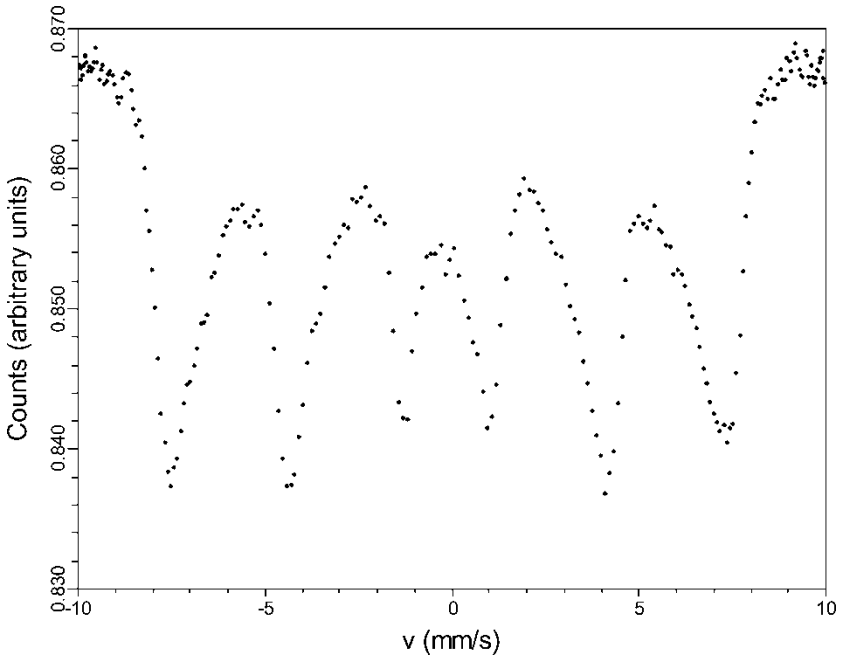

Figure 9. Mössbauer spectrum of magnetite polystyrene at 300 K.

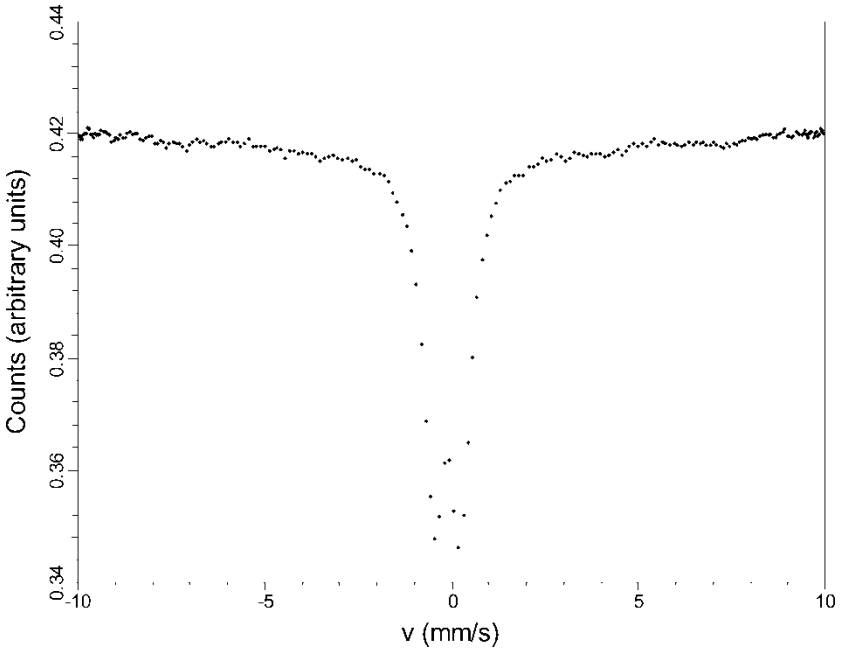

Figure 10. Mössbauer spectrum of magnetite polyester polystyrene at 300 K.

corresponding to Fe(III) in sublattice A, Fe(II) in sublattice B, and Fe(III) in sublattice B (21). As the particle size is reduced, the magnetization fluctuates rapidly along easy axes of magnetization and the six-line pattern starts distorting. The individual particles are in superparamagnetic domain; however, the interparticle interaction is strong enough to induce hyperfine splitting. The Brownian motion in the interacting particles induce line broadening. Finally, with further size reduction, a triplet corresponding to Fe(III) in octahedral and tetrahedral site and Fe(II) in octahedral site is observed (22). This is the superparamagnetic state of magnetite. In case of fine particles, the Fe(III) and Fe(II) in octahedral sites are difficult to distinguish and one often encounters a doublet (21).

Light scattering experiments showed that the majority of magnetite polystyrene and magnetite polyester polystyrene composite particles centered at a size of $\sim 10\,\mu m$.

During polymerization at elevated temperature, crystallization is inhibited in ambient conditions synthesis procedure in the presence of surfactants while on heating it is enhanced. When magnetite is grown in carboxylate functionalised polymers, its nucleation may be hindered due to formation of iron carboxylate complex. Carboxylate group facilitates the dispersion but hinders the crystallization (23). This may be responsible for lower magnetite content in polyester polystyrene as compared to polystyrene.

When polymerization is pursued at high temperature, the magnetite crystallites grow in size. The interparticle magnetic interactions enhance; therefore Mössbauer shows hyperfine splitting in spectrum. Results indicate that polymerization in ambient conditions helps in retaining the superparamagnetic property of the magnetite particles. Magnetite polyester polystyrene was used for solvent impregnation studies.

CMPO is a polar solvent, immiscible with aqueous phase. In the presence of diluent n-dodecane, its metal complex forms a third phase due to polar-polar interaction with aqueous medium and solubility in n-dodecane. This allows the extracted radionuclide to be separated into three phases therefore density separation methods are difficult to operate. A phase modifier, TBP is added to avoid the third phase formation (24). In order to evaluate the role of phase modifier and diluent on magnetic particles, CMPO loaded magnetic beads were prepared in different mixture proportions with TBP and n-dodecane. In one of the formulations (mixture type Ia, refer to Table 1), when the relative proportion of CMPO and TBP was maintained at 0.25:1.2 by moles and diluent was progressively reduced, the distribution coefficient was observed around 10. In the second formulation (mixture type Ib, refer to Table 1), where TBP and diluent concentrations were fixed and CMPO concentration was varied, the distribution coefficient remained around 10 for all the mixtures except when CMPO concentration was 1.5 M. Here, the distribution coefficient increased to 100. The trend of europium uptake is similar to uranium uptake demonstrated by Kaminsky and coworkers (25) using magnetic microparticles. The authors observed that 1.0 M CMPO in TBP impregnated on magnetite polymer composite gave one-order higher distribution coefficients for uranium than 0.1 M CMPO in TBP impregnated on magnetite polymer composite.

In the third formulation (mixture-type II, refer to Table 2), the phase modifier was not added. Only the CMPO concentration was increased. The relation between distribution coefficient and volume percent of CMPO in diluent is shown in Fig. 11. With the increase in CMPO, the K_d value increased. For concentration above 0.6 M CMPO (30% by volume), K_d values exceeded those obtained in combinations with TBP shown in Table 1. However, in the absence of diluent, CMPO showed diffusion limitations due to high viscosity (5×10^{-2} Pas (26)) into the pores of polyester polystyrene resin leading to significant reduction in K_d value.

In the vaporization method adopted for the fourth formulation (mixture-type III), the distribution coefficient increased to $\sim$1000. Ethanol presence allowed, by capillary action, the movement of CMPO into the pores of the polymer surface. On complete evaporation of ethanol, only CMPO remained as impregnated molecule causing enhancement of radionuclide sorption. The loading of the solvent on the beads was about 1% by weight as evaluated by difference in weights on initial and final washed product. Incorporating density and weight percent parameters, the volume equivalent of extractant was evaluated. For the removal of europium from waste

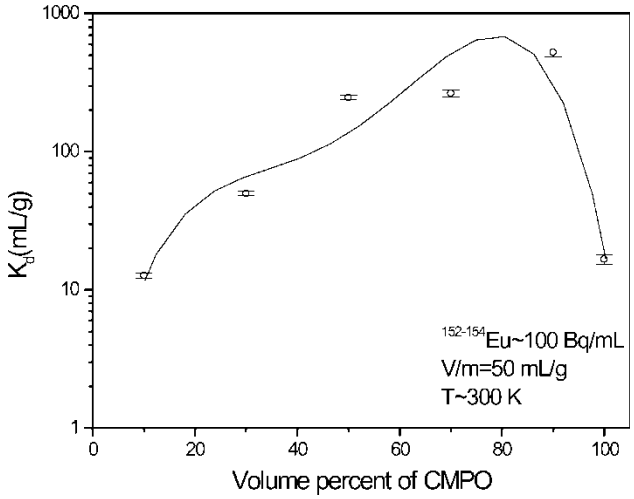

Figure 11. Distribution coefficient of Eu between sorbent and 2 N HNO_3 versus volume percent of CMPO in diluent (Error bar is added to the plot. Data fitted to fourth order polynomial).

solution ratio of 225×10^{-6}:1 of organic to aqueous by volume sufficed. A practical application of this volume ratio without support matrix is not possible in conventional separation systems based on density difference (27). The inventory of organic extractant volumes therefore significantly reduced by application of magnetic particles.

A variation of distribution coefficient with respect to europium concentration was studied to evaluate the saturation capacity of the magnetic sorbent for europium ions. The distribution coefficient versus europium concentration is shown in Fig. 12. As the concentration of europium is increased, the distribution coefficient increases. This effect was observed in accordance with the number of extractant sites available on the magnetic bead surface. After the surface is saturated with increasing europium concentration, a reduction in distribution coefficient is indicated. This behavior correlates to the Langmuir scheme of availability of finite sites for any reaction to be pursued on a surface (28). Kaminsky and coworkers (29) studied the sorption capability of ferromagnetic microparticles coated with CMPO using europium. Their studies also support the mechanism of monolayer adsorption. Yamaura and coworkers (30) studied the influence of variation in concentration of europium using CMPO impregnated on silanolized magnetite. CMPO-TBP mixture was loaded to the magnetic microparticles and distribution of europium on the bead with respect to aqueous medium was studied. The distribution coefficient for the europium concentration around 10^{-3} to 10^{-6} M was observed between 20–30. As compared

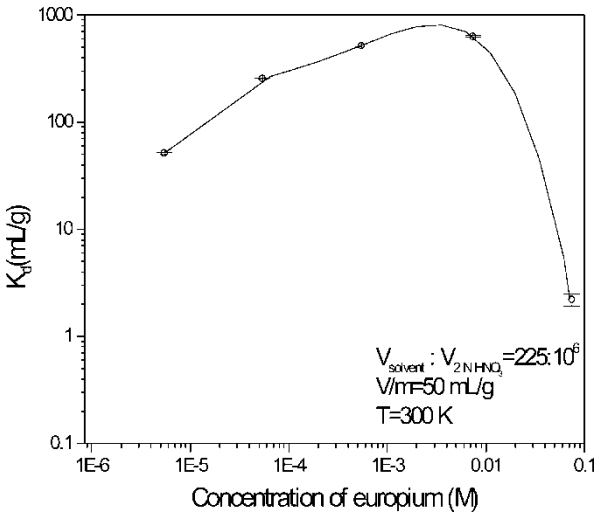

Figure 12. Distribution coefficient of Eu between sorbent and 2 N HNO_3 versus the concentration of Eu (M) (Error bar is added to the plot. Data fitted to fourth order polynomial).

to the silanolized surface the polyester polystyrene surface offered higher uptake for CMPO and therefore for europium. The silinaol surface offers a covalent binding site to CMPO while polyester polystyrene offers polar interactions for binding of CMPO. Due to covalent bonding, the directional specificity of CMPO towards europium is changed. When polar interactions allow binding, the directional specificity towards europium is unchanged and therefore higher extraction efficiency is observed. A similar investigation on magnetite polymer composites by Nunez and coworkers (31) indicated that polar functionalized magnetic particles such as acryl amide based polymer composites with magnetite have higher sorption capablity for CMPO based solvent than divinyl benzene polymer, polyacrolein polymer, styrene divinyl benzene polymer and dextran polymer, composites with magnetite.

CONCLUSIONS

For the preparation of magnetite based solvent extractant, iron stoichiometry and polymerization temperatures were controlled to obtain superparamagentic Fe_3O_4 coated with polymer. Maximum impregnation of CMPO on polymer interface was observed when the evaporation method was adopted as a method of contacting. Absence of diluents and phase modifiers is a significant advantage observed towards low inventory utilization of valuable solvents for radionuclide separation techniques.

ACKNOWLEDGEMENTS

The authors thank Dr. S.M. Yusuf, Solid State Physics Division, Bhabha Atomic Research Center for magnetisation data. Ms. Ambashta thanks Dr. R.R. Chitnis of Back End Technology Development Division, Bhabha Atomic Research Center for his suggestions on solvent impregnation.

REFERENCES

1. Nuñez, L., Buchholz, B.A., Ziemer, M., et al. (1994) *Argonne National Laboratory Report*; ANL-94/97.
2. Nuñez, L., Buchholz, B.A., and Vandegrift, G.F. (1995) *Separation Science and Technolgy*, 30 (7–9): 1455.
3. Ebner, A.D., Ritter, J.A., and Nunez, L. (1999) *Separation Science and Technology*, 34 (6–7): 1333.
4. Hatch, G.P. and Stelter, R.E. (2001) *Journal of Magnetism and Magnetic Materials*, 225: 262.
5. Dresco, P.A., Zaitsev, V.S., Gambino, R.J., and Chu, B. (1999) *Langmuir*, 15: 1945.
6. Horwitz, E.P., Kalina, D.G., Kaplan, L., et al. (1982) *Separation Science & Technology*, 17: 1261.
7. Schulz, W.W. and Horwitz, E.P. (1988) *Separation Science and Technology*, 23: 1191.
8. Mathur, J.N. and Nash, K.L. (1998) *Solvent Extraction and Ion exchange*, 16 (6): 1341.
9. Nunez, L., Kaminski, M.D., Bradley, C., et al. (1995) *Argonne National Laboratory Report*; ANL-95/1.
10. Regazzoni, A.E., Urrutia, G.A., Blesa, M.A., et al. (1981) *Journal of Inorganic and Nuclear Chemistry*, 43: 1489.
11. Dresco, P.A., Zaitsev, V.S., Gambino, R.J., et al. (1999) *Langmuir*, 15 (6): 1975.
12. Massart, R. (1981) *IEEE Transactions on Magnetics*; Mag-17: 1247.
13. Klug, H.P. and Alexander, L.E. (1981) *X-ray diffraction Procedures for Polycrystalline and Amorphous Materials*; John Wiley & Sons, Inc., 89.
14. Heimendahl, M.V. (1970) *Electron Microscopy of materials: An introduction*; Academic Press, Inc. (London) Ltd., 95.
15. Gribanov, N.M., Bibik, E.E., Buzunov, O.V., et al. (1990) *Journal of Magnetism and Magnetic Materials*, 85: 7.
16. Gokon, N., Shimada, A., Kaneko, H., et al. (2002) *Journal of Magnetism and Magnetic Materials*, 238: 47.
17. Tamaura, Y., Yoshida, T., and Katsua, T. (1984) *Bulletin Chemical Society of Japan*, 57: 2411.
18. Kiyama, M. (1974) *Bulletin of Chemical Society of Japan*, 47: 1646.
19. Suslick, K.S. and Price, G.J. (1999) *Annual Reviews in Material Science*, 29: 295.
20. Hou, Y., Yu, J., and Gao, S. (2003) *Journal of Materials Chemistry*, 13: 1983.
21. Hartridge, A., Bhattacharya, A.K., Sengupta, M., et al. (1997) *Journal of Magnetism and Magnetic Materials*, 176: L89.
22. Hayashi, M., Susa, M., and Nagata, K. (1997) *Journal of Magnetism and Magnetic Materials*, 171: 170.

23. Bee, A., Massart, R., and Neveu, S. (1995) *Journal of Magnetism and Magnetic Materials*, 149: 6.
24. Carlson, T.E., Chipman, N.A., and Wai, C.M. (1996) *Separation Techniques in Nuclear Waste Management*; CRC Press, 3.
25. Kaminsky, M.D. and Nunez, L. (2000) *Separation Science and Technology*, 35 (13): 2003.
26. Takeshit, K., Takashima, Y., Matsumoto, S., et al. (1995) *Journal of Chemical Engineering of Japan*, 28 (10): 91.
27. Lumetta, G.J., Wester, D.W., Morrey, J.R., et al. (1993) *Solvent Extraction and Ion Exchange*, 11 (4): 663.
28. Renard, V., Ivanchenko, V.A., Chizhov, A.A., et al. (1994) *Journal of Alloys and Compounds*, 213/214: 545.
29. Kaminsky, M., Landsberger, S., Nunez, L., et al. (1997) *Separation Science and Technology*, 32 (1–4): 115.
30. Yamaura, M., Camilo, R.L., and Felinto, M.C.F.C. (2002) *Journal of Alloys and Compounds*, 344: 152.
31. Nunez, L. and Kaminski, M.D. (1999) *Journal of Magnetism and Magnetic Materials*, 194: 102.